Rotation–vibration interactions in formaldehyde: Results for low vibrational excitations

Mutsumi Aoyagi and Stephen K. Gray

Citation: The Journal of Chemical Physics **94**, 195 (1991); doi: 10.1063/1.460698
View online: http://dx.doi.org/10.1063/1.460698
View Table of Contents: http://scitation.aip.org/content/aip/journal/jcp/94/1?ver=pdfcov
Published by the AIP Publishing

Rotation–vibration interactions in formaldehyde: Results for low vibrational excitations

Mutsumi Aoyagi[a] and Stephen K. Gray
Theoretical Chemistry Group, Chemistry Division, Argonne National Laboratory, Argonne, Illinois 60439

(Received 23 April 1990; accepted 18 September 1990)

We have carried out large-scale variational calculations on formaldehyde including all six vibrational modes and the rotational mode associated with K (the projection of total angular momentum on a body-fixed axis). A complete form of the Watson Hamiltonian and a realistic potential function based on *ab initio* data are used. Emphasis in this paper is placed on the low vibrational energy regime and the effect of Coriolis interaction. Comparison is made with other theoretical calculations and experiment, where available. Analysis of some of our full mode rovibrational states shows instances of simultaneous vibration and rotation mixing due to a strong a-axis Coriolis interaction. We show that such mixing can be understood from the perspective of a classical nonlinear resonance between the rotational frequency and the difference in two bending mode (out-of-plane and in-plane) frequencies. This confirms previous full dimension classical and reduced dimension quantum studies and represents an alternative way of understanding Coriolis interaction in the low vibrational energy regime.

I. INTRODUCTION

The dynamics of vibration–rotation interaction in polyatomic molecules has been intensely studied over the past few years. A number of experimental and theoretical studies have shown that rotation plays an important role in the intramolecular redistribution of energy and collisional energy transfer.[1–11] One of the most interesting conclusions of such studies is that the picture in which vibrational and rotational motion are nearly separable degrees of freedom is an oversimplification in the high total angular momentum regime. The stimulated emission pumping (SEP) experiments of Dai *et al.*[1] have shown that a mechanism of rotation induced vibrational mixing is crucial to interpret their SEP spectra of ($X\,^1A_1$) formaldehyde with moderate vibrational excitation and varying degrees of rotational excitation ($E_{\rm vib} = 7000$–$9000\,{\rm cm}^{-1}$, $J = 10$–16; $E_{\rm vib}$ denotes vibrational energy relative to zero-point energy). As total angular momentum J is increased, both vibration and rotation mixings occur that lead to difficulties in assigning spectral lines. To understand such results, it is necessary to carry out more extensive theoretical calculations than the usual simple arguments based on the low-order perturbation theory. There have been several recent theoretical studies of rovibrational coupling in formaldehyde. Burleigh *et al.*[4] have investigated the rovibrational dynamics of formaldehyde in a reduced dimension model and have shown that an analysis using Coriolis adapted normal modes leads to a simple picture of the dynamics. Gray and Davis[6] have studied the effects of rotation on the intramolecular redistribution of energy in formaldehyde by carrying out classical trajectory calculations on a full dimension model, as well as on a reduced dimension one. They found that the breakdown of K as a constant of the motion (K mixing), along with the breakdown of individual normal mode states, could occur even in the lower vibrational states due to a classical nonlinear resonance effect involving the rotational frequency and a difference in vibrational frequencies. Recently Sibert[5] has studied the mechanism of rotationally induced vibrational mixing in the $K = J$ limit for vibrational excitations up to $8600\,{\rm cm}^{-1}$ by using almost-degenerate perturbation theory. He found that a combination of a axis Coriolis and Fermi couplings can lead to extensive vibrational mixing.

In this paper, we perform large scale variational calculations on formaldehyde using a realistic *ab initio* potential function. Our focus here will be on the low vibrational excitation regime ($E_{\rm vib} < 5000\,{\rm cm}^{-1}$), but with varying degrees of rotational excitation. We will also examine the role of Coriolis interaction in these states. One might question the necessity of such a heavy-handed approach in relation to a regime where it could be argued the spectroscopy is relatively well understood. We should therefore note three important reasons for the present study. First, we wish to show that standard variational (or vibrational configuration interaction) methods can indeed be applied to large scale rovibrational problems such as formaldehyde with the aid of iterative diagonalization techniques borrowed from electronic structure theory. (Actually, a preliminary account of this approach for the $J = 0$ states of formaldehyde has already been discussed.)[12] It should be noted that our calculations represent the most accurate, completely *a priori* (and nonperturbative) estimates of the vibration–rotation eigenstates of formaldehyde in this regime. These results therefore serve as benchmarks upon which other calculations and methods may be gauged. Also, since our results represent excellent approximations to the true eigenstates of the potential function, comparison with experiment will show up inadequacies in the potential function and point to the need for improvements. Second, we wish to show that some consequences of Coriolis interaction in the full mode quantum

[a] Present address: Basic Research Division, National Chemical Laboratory for Industry, Tsukuba, Ibaraki 305, Japan.

 0021-9606/91/010195-13$03.00

states can indeed be understood with the classical nonlinear resonance idea of Davis and Gray.[6] This leads to a novel perspective on well-known spectroscopic features such as accidental Coriolis interaction. The third reason for this study is that it represents a first step towards understanding the higher vibrational energy regime. In future work it will be possible to borrow some of the methods and ideas presented here for understanding the much more difficult (and more interesting) regime involving both significant vibrational and rotational excitation.

In Sec. II we present the Hamiltonian, basis functions, and some details of our variational calculations. Section III A discusses the rotationless ($J=0$) vibrational energy levels and compares our results to other theoretical results, as well as experiment. Section III B presents our results for rotationally excited formaldehyde, focusing on the 4_1 and 4_2 vibrational states. Section III C presents a more detailed theoretical explanation of the vibration and rotation mixing seen in the 4_2 vibrational state in terms of a resonance mechanism analogous to that proposed earlier by Gray and Davis.[6] Section III C also includes comparison of the full dimension results with a new reduced dimension model. Finally, Sec. IV concludes with a brief summary and discussion of future research directions.

II. METHOD OF CALCULATION

A. Hamiltonian and primitive basis functions

The method used in this study is based on the work of Whitehead and Handy.[13] We use the vibration–rotation Hamiltonian in the form given by Watson:[14]

$$H = 1/2 \sum_{\alpha\beta} \mu_{\alpha\beta}(J_\alpha - \Pi_\alpha)(J_\beta - \Pi_\beta) + 1/2 \times \sum_k (P_k^2 + \omega_k^2 Q_k^2) + V(Q) - 1/8\hbar^2 \sum_\alpha \mu_{\alpha\alpha}. \quad (1)$$

Here Latin indices denote normal modes and Greek indices denote the body-fixed axes (x,y,z) which correspond to the (c,b,a) axes associated with the principal axes of the molecule. The a or z axis corresponds, at equilibrium, to the CO axis. In Eq. (1), J is the total angular momentum vector in a body-fixed Eckart frame, (Q_k, P_k) are the normal coordinates and their conjugate momenta, and $V(Q)$ is the anharmonic part of the potential energy function. The inverse moment of inertia tensor μ depends on the normal coordinates and can be Taylor series expanded in the Q_k's. We use a fourth-order expression for μ. The vibrational angular momentum Π is given by

$$\Pi_\alpha = \sum_{kl} \zeta_{kl}^\alpha Q_k P_l, \quad (2)$$

where the ζ_{kl}^α's are the Coriolis coefficients, which are obtained from the normal mode eigenvectors of the potential function. For the purposes of analysis later on we may rewrite Eq. (1) as

$$H = H_{\rm vib} + H_{\rm rot} + W. \quad (3)$$

In Eq. (3), $H_{\rm vib}$ denotes the vibrational Hamiltonian, which includes anharmonicity, vibrational angular momentum and the quantum mechanical Watson term:

$$H_{\rm vib} = 1/2 \sum_k (P_k^2 + \omega_k^2 Q_k^2) + V(Q) + 1/2 \sum_{\alpha\beta} \mu_{\alpha\beta}\Pi_\alpha\Pi_\beta - 1/8\hbar^2 \sum_\alpha \mu_{\alpha\alpha}. \quad (4)$$

$H_{\rm rot}$ is the asymmetric rotor Hamiltonian which also includes centrifugal effects, i.e., the variation of $\mu_{\alpha\beta}$ with Q,

$$H_{\rm rot} = 1/2 \sum_{\alpha\beta} \mu_{\alpha\beta} J_\alpha J_\beta, \quad (5)$$

and W is the Coriolis interaction term

$$W = -\sum_{\alpha\beta} \mu_{\alpha\beta} J_\alpha \Pi_\beta. \quad (6)$$

All parameters in the Hamiltonian, except the potential energy function, are summarized in Table I. The potential energy function employed is an eighth-order normal coordinate expansion, based on *ab initio* data, due to Sibert (Ref. 5 and personal communication). This potential function is superior to the one originally given by Romanowski and coworkers[15] in that spurious behavior at moderate vibrational excitation energies is absent.[5]

In the case of $J=0$ we employ a simple product of Hermite–Gaussian functions $\chi_{n_k}(Q_k)$[13] as our zero-order functions and calculate variationally the vibrational eigenfunctions Φ_i of $H = H_{\rm vib}$:

$$\Phi_i = \sum_{N<N_{\max}} C_{\mathbf{n}}^i \chi_{n1}(Q_1)\chi_{n2}(Q_2)\cdots\chi_{n6}(Q_6), \quad (7)$$

where $\mathbf{n} = (n_1, n_2, \ldots, n_6)$ denotes the zero-order normal mode vibrational quanta, $N = n_1 + n_2 + \cdots + n_6$, and $N_{\max}$ is a maximum value for N. (See Sec. II C below for a brief discussion of how the variational calculations are actually performed.)

In the case of rotationally excited formaldehyde, a straightforward extension of the method described above for the $J=0$ problem is employed. We use a simple product of Hermite–Gaussian functions $\chi_{n_k}(Q_k)$ and "Wang-type" rotational functions[16] $R_{J,K}^{+/-}$ as our zero-order functions. The eigenfunctions with total angular momentum J can be written as

$$\Psi_J = \sum_{N<N_{\max}} \sum_{K<J} C_{\mathbf{n}K} \chi_{n1}(Q_1)\chi_{n2}(Q_2)\cdots\chi_{n6}(Q_6) R_{J,K}^{+/-}, \quad (8)$$

where the summation over K includes both R_{JK}^+ and R_{JK}^- functions. The Wang-type rotational functions $R_{J,K}^{+/-}$ we employ are those suggested and discussed by Huber[16] and recently used by Burleigh and co-workers.[4] They are related to spherical harmonic functions $Y_{J,K}$ by

$$\begin{aligned} R_{JK}^+ &= (1/2)^{-1/2}(Y_{J,K} + (-1)^K Y_{J,-K}), \\ R_{JK}^- &= -i(1/2)^{-1/2}(Y_{J,K} - (-1)^K Y_{J,-K}), \\ R_{J,-K}^{+/-} &= (+/-)(-1)^K R_{J,K}^{+/-}; \quad K \geqslant 0. \end{aligned} \quad (9)$$

The functions defined by Eq. (9) consist of R_{J0}^+ and the $2J$ functions $R_{JK}^{+/-}$ ($R_{J0}^- = 0$). Huber has presented a scheme involving ladder operators to evaluate matrix elements involving these functions.[16] Note the latter part of Eq. (9) is the "wrap around" condition and must be carefully applied after the evaluation of the cumulative effect of all relevant

TABLE I. Hamiltonian parameters.[a]

Harmonic frequencies			
Mode k	Symmetry	ω_k (cm^{-1})	Description
1	A_1	2937.428	CH symmetric stretch
2	A_1	1777.801	CO stretch
3	A_1	1543.958	HCH bend
4	B_1	1188.312	out-of-plane bend
5	B_2	3012.051	CH asymmetric stretch
6	B_2	1269:429	in-plane wag

Inverse moment of inertia and Coriolis coefficient				
α	k	l	$\mu^0_{\alpha\alpha}$ (cm^{-1})	ζ^{α}_{kl}
a	4	5	19.1522	0.852 097
	4	6		−0.523 385
b	1	4	2.6067	−0.506 904
	2	4		−0.610 299
	3	4		−0.608 756
c	1	5	2.2945	0.033 349
	1	6		0.914 217
	2	5		0.512 812
	2	6		0.331 178
	3	5		0.857 853
	3	6		−0.233 514

Expansion coefficients of the inverse moment of inertia (k = normal mode number)			
α	β	k	$a^{\alpha\beta}_k$(amu$^{1/2}$ Å)
a	a	1	−2.266 849
a	a	2	0.693 124
a	a	3	1.192 697
b	b	1	−0.829 323
b	b	2	5.379 227
b	b	3	−4.702 300
c	c	1	−3.096 173
c	c	2	6.072 351
c	c	3	−3.509 603
b	c	5	1.303 003
b	c	6	2.121 356

[a] Results from Romanowski, Bowman, and Harding (Ref. 15). For the sake of brevity, only the first order terms in μ are listed, although our calculations actually included terms up to fourth order.

ladder operators. Use of this Wang basis set allows us to treat real symmetric Hamiltonian matrices, as opposed to the complex Hermitian ones that would result if the spherical harmonic functions were used directly.

For the $J \neq 0$ problems, a complete set of $2J+1$ $R^{+/-}_{J,K}$ functions ($K = 0, 1, \ldots, J$) must, in principle, be used to describe rovibrational states with total angular momentum J. However we have found that the expansion of rotational part of the wave function in Eq. (8) can be truncated to a more compact set ($K = 0,1, \ldots, K_{\max}$), since we are interested in only lower magnitude K states with a high J quantum number. It should be noted that there is no direct coupling between K states with ΔK greater than 2. Therefore, Wang zero-order states which are widely separated in K are very weakly coupled through high order interactions.

B. An alternative zero-order description of rovibrational states

A major concern of this paper is the effect of Coriolis interaction in inducing vibration and rotation mixing. While the actual diagonalization to obtain the full rovibrational eigenstates involves the expansion Eq. (8) in terms of primitive normal-mode/Wang states, it will prove useful to re-express the corresponding full rovibrational states in terms of a different zero-order basis that already includes the effects of molecular asymmetry (through $H_{\rm rot}$) and anharmonicity (through V). Specifically, we also diagonalized the Hamiltonian

$$H_0 = H - W = H_{\rm vib} + H_{\rm rot} \tag{10}$$

to obtain a new zero-order basis set Ψ^0_J. An expansion similar to Eq. (8) applies:

$$\Psi^0_J = \sum_{N<N_{\max}} \sum_{K<J} D_{nK} \chi_{n1}(Q_1)\chi_{n2}(Q_2)\cdots\chi_{n6}(Q_6) R^{+/-}_{J,K},$$

or, more abstractly,

$$|\Psi^0_J\rangle = \sum_{N<N_{\max}} \sum_{K<J} D_{nK} |J;K+/-\rangle |n_1,n_2,n_3,n_4,n_5,n_6\rangle, \tag{11}$$

where an obvious ket notation has been introduced to indi-

cate the primitive normal mode/Wang states. For the low vibrational excitations of interest here, usually just one primitive ket will dominate each $|\Psi_J^0\rangle$. A $|\Psi_J^0\rangle$ state that is dominated by a particular primitive ket $|K+/-\rangle|n_1, n_2, n_3, n_4, n_5, n_6\rangle$ will be labeled as $|K+/-\rangle|n_1, n_2, n_3, n_4, n_5, n_6)$, with the soft brackets to remind the reader that other primitive states might be involved through molecular asymmetry and anharmonicity effects. Table II displays the primitive decompositions of a few selected $|\Psi_J^0\rangle$ states. Note that the major coupling effect, at these low vibrational excitations, is molecular asymmetry, although anharmonicity effects can be seen in some instances.

C. Program system developed for the present study

In the case of our $J=0$ calculations, we used a set of $\sim 12\,000$ zero-order (primitive) basis functions for each C_{2v} symmetry of Eq. (7). In the case of our $J \neq 0$ calculations we used $\sim 20\,000$ functions in the expansion of Eq. (8). (For $J \neq 0$, Coriolis coupling, of course, mixes different vibrational symmetries.) In order to generate and diagonalize such large Hamiltonian matrices a new program for the calculation of vibration–rotation states has been developed. Since the potential is a normal coordinate expansion, it proved to be convenient to evaluate the matrix elements with ladder operators, as suggested in the work of Huber.[16] More importantly, we have developed a new diagonalization program specialized for use in large scale vibration–rotation problems. In this program, we use an iterative diagonalization method due to Davidson,[17] which has been widely used in the field of electronic structure. This method does not require as much core memory as methods typically used in the field of rovibrational analysis. In this method, one solves iteratively for only the first M eigenstates, as opposed to solving for all the eigenstates. Typically $M \sim 200$ in our applications. We should also note that the Lanczos method,[18,19] which is similar in spirit to the iterative method we employ, has also been successfully used to calculate vibrational eigenstates. All calculations were carried out on an Alliant FX/8 minisupercomputer. CPU times required to calculate Hamiltonian matrix elements and to diagonalize were typically 1.5 and 6 h, respectively.

III. CORIOLIS INTERACTIONS OF LOW-LYING ROVIBRATIONAL STATES

A. Vibrational energy levels up to 5000 cm^{-1} above the ground vibrational state

In this section, we will present results for the low-lying vibrational energy states ($J=0$) up to about 5000 cm^{-1} above the zero-point energy. This information is complementary to our previously reported $J=0$ results[12] which were concerned with higher vibrational excitation energies. Calculations have been performed with $N_{\max}=6$ to 14. The $N_{\max}=14$ case consists of about 12 000 zero-order basis functions in each symmetry (a_1, a_2, b_1, and b_2). Comparison of the $N_{\max}=14$ and 12 results suggests that our best results ($N_{\max}=14$) are converged to less than 1 cm^{-1} for energies less than 5000 cm^{-1}. The calculated vibrational energy levels of the present study and other theoretical studies, along with available experimental data, are summarized in Table III. The column headed by SCF-CI represents the results of self-consistent field–configuration interaction calculations of Romanowski and co-workers.[15] The column headed by PT(6) represents the sixth-order perturbation theory results of Sibert.[5] It can be seen that the present variational results and the PT(6) results agree reasonably well, with differences usually much less than one or two cm^{-1}. These results differ a little more significantly with the SCF-CI results owing to our and Sibert's use of an improved potential ener-

TABLE II. Primitive basis decompositions of selected[a] eigenstates of H_0 for $J=16$.

State label[b]	Energy[c]/cm^{-1}	Decomposition[d]
$\|0)\|000100)$	1497.0	$0.92\|0\rangle\|000100\rangle + 0.36\|2+\rangle\|000100\rangle$
$\|2-)\|000001)$	1618.2	$0.98\|2-\rangle\|000001\rangle + 0.10\|4-\rangle\|000001\rangle$
$\|2+)\|000001)$	1624.0	$0.92\|2+\rangle\|000001\rangle - 0.36\|0\rangle 000001\rangle$
$\|4-)\|000100)$	1636.9	$0.99\|4-\rangle\|000100\rangle - 0.10\|2-\rangle\|000100\rangle$
$\|4+)\|000100)$	1636.9	$0.99\|4+\rangle\|000100\rangle - 0.10\|2+\rangle\|000100\rangle$
$\|3-)\|000101)$	2937.7	$0.98\|3-\rangle\|000101\rangle - 0.13\|1-\rangle\|000101\rangle$
$\|3+)\|000101)$	2938.2	$0.97\|3+\rangle\|000101\rangle - 0.18\|1+\rangle\|000101\rangle$
$\|5-)\|000200)$	2870.5	$0.98\|5-\rangle\|000200\rangle + 0.15\|5-\rangle\|200000\rangle$
$\|5+)\|000200$	2870.5	$0.98\|5+\rangle\|000200\rangle + 0.15\|5+\rangle\|100000\rangle$
$\|3-)\|000002)$	2910.6	$0.9713-\rangle\|000002\rangle - 0.13\|1-\rangle\|000002\rangle + 0.13\|3-\rangle\|100000\rangle$
$\|3+)\|000002)$	2911.1	$0.95\|3+\rangle\|000002\rangle + 0.17\|1+\rangle 000002\rangle - 0.13\|3+\rangle\|100000\rangle$
$\|5-)\|000101)$	2971.0	$0.99\|5-\rangle\|000101\rangle$
$\|5+)\|000101)$	2971.0	$0.99\|5+\rangle\|000101\rangle$

[a] States grouped together are in different energy regimes. There can be many states between these regimes which we have chosen not to display.
[b] The $J=16$ label has been suppressed. Thus $|2-)|000001) \equiv |16;2-)|000001)$.
[c] Energy relative to the vibrational ground state of H_0 with $J=0$, $E=5778.9$ cm^{-1} (zero-point energy).
[d] Only primitive basis set components $|C|>0.10$ are displayed.

TABLE III. Theoretical and experimental energy levels (cm^{-1}) of the low-lying vibrational states of $X\,^1A_1$ formaldehyde ($J=0$). Energies are relative to the zero-point energy, (5778.8 cm^{-1} in the present calculations).

State[a]	Sym	SCF-CI[b]	Pert-6[c]	Present[d]	Expt.[e]
4_1	b_1	1160.4	1166.1	1166.1	1167.3
6_1	b_2	1245.4	1250.5	1250.5	1249.0
3_1	a_1	1500.1	1505.7	1505.7	1500.2
2_1	a_1	1747.1	1747.4	1747.4	1746.0
4_2	a_1	2314.9	2323.2	2323.1	2327.1
$4_1 6_1$	a_2	2415.3	2426.2	2426.0	···
6_2	a_1	2488.8	2497.8	2497.6	···
$3_1 4_1$	b_1	2654.8	2667.7	2667.6	2655.5
$3_1 6_1 + 5_1$	b_2	2700.1	2726.6	2725.6	2719.2
1_1	a_1	2781.3	2780.6	2780.0	2782.5
$5_1 - 3_1 6_1$	b_2	2856.9	2845.4	2845.9	2843.3
$2_1 4_1$	b_1	2898.9	2905.8	2905.6	2905
$2_1 6_1$	b_2	3002.5	3001.9	3002.4	3000.1
3_2	a_1	2997.2	3009.8	3009.9	2999.5
$2_1 3_1$	a_1	3239.6	3245.8	3245.8	3238.5
4_3	b_1	3456.3	3469.6	3470.8	···
2_2	a_1	3478.6	3475.9	3475.9	3471.7
$4_2 6_1$	b_2	3575.1	3590.1	3589.8	···
$4_1 6_2$	b_1	3667.5	3684.4	3683.5	···
6_3	b_2	3726.5	3741.9	3741.4	···
$3_1 4_2$	a_1	3801.5	3820.5	3820.2	3825.5
$3_1 4_1 6_1 + 4_1 5_1$	a_2	3847.8	3894.5	3893.3	···
$1_1 4_1$	b_1	3913.7	3938.1	3937.9	···
$3_1 6_2 + 5_1 6_1$	a_1	3898.0	3945.8	3943.2	···
$4_1 5_1 - 3_1 4_1 6_1$	a_2	3995.2	3999.4	4000.7	···
$1_1 6_1$	b_2	4004.4	4024.7	4024.3	···
$2_1 4_2$	a_1	4043.4	4054.8	4054.4	···
$5_1 6_1 - 3_1 6_2$	a_1	4083.4	4088.3	4089.0	4093
$3_2 4_1$	b_1	4146.1	4167.5	4167.2	···
$2_1 4_1 6_1$	a_2	4160.0	4168.1	4168.3	···
$3_2 6_1 + 3_1 5_1$	b_2	4145.8	4206.0	4204.5	···
$2_1 6_2$	a_1	4229.6	4250.9	4251.5	···
$1_1 3_1$	a_1	4268.3	4258.5	4258.9	4260
$3_1 5_1 - 3_2 6_1$	b_2	4346.8	4342.7	4343.8	4350
$2_1 3_1 4_1$	b_1	4385.2	4400.0	4399.6	···
$2_1 3_1 6_1 + 2_1 5_1$	b_2	4459.3	4475.1	4474.6	···
3_3	a_1	4499.2	4511.3	4511.3	···
$1_1 2_1$	a_1	4528.9	4528.7	4528.1	4528
$2_1 5_1 - 2_1 3_1 6_1$	b_2	4581.0	4575.4	4575.4	···
$4_4 + 1_1 4_2$	a_1	4623.5	4609.0	4609.0	4629.8
$2_2 4_1$	b_1	4621.4	4626.5	4626.1	···
$2_2 6_1 - 2_1 5_1$	b_2	4746.0	4737.5	4738.4	4734.8
$2_1 3_2$	a_1	4729.5	4742.3	4742.2	···
$4_3 6_1$	a_2	4718.6	4743.4	4743.1	···
$4_2 6_2$	a_1	4833.2	4854.6	4853.7	···
$4_1 6_3$	a_2	4915.0	4941.4	4939.2	···
$3_1 4_3$	b_1	4934.0	4963.8	4963.2	···
$2_2 3_1$	a_1	4964.4	4966.7	4966.6	···
$6_4 + 1_1 6_2$	a_1	4983.8	4983.6	4982.3	···

[a] State assignments are made from the present results. Labels of basis functions which has more than 10% contribution to the total wavefunction, i.e., $C^2 > 0.1$, are listed in decreasing order.
[b] Results from Romanowski, Bowman, and Harding (Ref. 15).
[c] Results of sixth-order Van Vleck perturbation theory calculations by Sibert (Ref. 5).
[d] Variational results using $N_{max} = 14$. Hamiltonian matrix dimensions of each symmetry are 11 628(a_1), 7812(a_2), 8232(b_1), and 11 088(b_2), respectively.
[e] Experimental results from Reisner, Field, Kinsey, and Dai (Ref. 20).

gy surface fit. (See Sec. II A.) Thus the SCF-CI results tend to differ more significantly from the present results as energy increases. There is also reasonable agreement between the present and experimental results.[20] However, occasional differences between experiment and theory on the order of 10 or 20 cm^{-1} are seen, pointing to the necessity of further refinements to the potential surface. In the Sec. II B, we will present results for the rotationally excited states near the 4_1 and 4_2 vibrational levels.

Recall (Sec. II A and Table I) that we used a fourth-order expansion formula of μ to accurately include centrifugal effects. We find, however, that these effects are less important compared with other effects such as a-axis Coriolis and anharmonic effects, as far as low-lying states are concerned. For example, level shifts less than 0.5 cm^{-1} were seen when we performed the equivalent calculations with the moment of inertia tensor taken to be diagonal and independent of the normal coordinates.

B. Rotational levels of 4_1 and 4_2 vibrational states

A full calculation of the rotationally excited states as described in Sec. II A, with $N_{max} = 14$ is not possible at the present stage owing to the very large matrix sizes involved. Since in this subsection we are concerned with the 4_1 and 4_2 vibrational states, one can expect, however, that these states are essentially converged with N_{max} less than $N_{max} = 14$. Table IV displays the lowest lying vibrational levels (with $J = 0$) obtained by employing various basis set sizes N_{max}. As seen from Table IV, the convergence with basis set size is quite smooth and deviations of less than 2.0 cm^{-1} from the fully converged values ($N_{max} = 14$) are obtained by $N_{max} = 6$. Rotational energy levels with $J = 4$ are thus calculated using the vibrational basis sets with $N_{max} = 6$ and the complete rotational basis set ($K_{max} = J$, see Sec. II). The calculated results and available experimental data are summarized in Table V. A number of experimental studies[21,22] have been carried out to analyze the strong a-axis Coriolis interaction between ν_4 and ν_6 bands, and they have provided a complete set of rotational constants. It is an important check of the present results to compare our calculated rotational levels with the experimentally inferred values. It can be seen that the theoretical and experimental results are in quite reasonable agreement for our purposes. Note, however, that differences on the order of 2 cm^{-1} can be seen in some of the larger K states. Such differences are due to small inadequacies in the theoretical inverse moment of inertia, as well as the Coriolis coupling coefficients, which are all ultimately due to inadequacies in the potential surface.

The $J = 16$ rovibrational states of interest were obtained with $N_{max} = 6$ and $K_{max} = 10$. Table VI presents various rotational excitations associated with the 4_1 and 4_2 vibrational states. In Table VI we have chosen to display only those rotational excitations dominated by a K^+ Wang state. It turns out that there is always a nearby rovibrational eigenstate dominated by a K^- Wang state that is of similar (but not identical) character, which we choose not to display here. Actually, the K^+ dominated rovibrational eigenstates always show slightly more rovibrational mixing than the K^- dominated states, and this is another reason for our displaying these states. Table VI also presents the decomposition of our full eigenstates in terms of the new zero-order states, i.e., the eigenfunctions of H_0 (see Sec. II B). Let us first consider the 4_1 rovibrational states. Despite the apparent purity of these states—the coefficient for the major zero-order component is always 0.85 or larger—two a-axis Coriolis effects should be noted. First one has what might be called standard a-axis Coriolis interaction: zero-order states $|K+/-)|\ldots,n_4,\ldots,n_6)$ can mix with states $|K-/+)|\ldots,n_4+/-1,\ldots,n_6+/-1)$ because W connects the major primitive components $|K+/-\rangle|\ldots, n_4,\ldots,n_6\rangle$ and $|K-/+\rangle|\ldots,n_4+/-1,\ldots,n_6+/-1\rangle$. Thus, for example, the full rovibrational state in the 4_1 band that we label $K = +2$ involves not only $|2+)|000100)$ but

TABLE IV. Convergence[a] of the vibrational energy levels[b] (cm^{-1}) with respect to basis set size.

State Sym		N_{max} = 4	6	8	12
Gr.	a_1	5779.2(0.4)	5778.9(0.1)	5778.8(0.0)	5778.8
4_1	b_1	1167.9(1.8)	1166.4(0.3)	1166.1(0.0)	1166.1
6_1	b_2	1252.5(2.0)	1250.8(0.3)	1250.5(0.0)	1250.5
3_1	a_1	1508.1(2.4)	1506.0(0.3)	1505.7(0.0)	1505.7
2_1	a_1	1750.7(3.3)	1747.7(0.3)	1747.4(0.0)	1747.4
4_2	a_1	2352.3(29.2)	2323.7(0.6)	2323.2(0.0)	2323.1
$4_1 6_1$	a_2	2454.3(28.3)	2426.5(0.5)	2426.0(0.0)	2426.0
6_2	a_1	2525.8(28.2)	2498.1(0.5)	2497.6(0.0)	2497.6
$3_1 4_1$	b_1	2696.1(28.5)	2668.2(0.6)	2667.7(0.1)	2667.6
$3_1 6_1$	b_2	2749.8(24.2)	2726.5(0.9)	2725.7(0.1)	2725.6
1_1	a_1	2797.0(17.0)	2781.9(1.9)	2780.2(0.2)	2780.0
5_1	b_2	2867.0(21.1)	2847.4(1.5)	2846.0(0.1)	2845.9
$2_1 4_1$	b_1	2938.7(33.1)	2906.3(0.7)	2905.7(0.1)	2905.6

[a] Differences of each level from converged values ($N_{max} = 12$) are given in parentheses.
[b] After the ground state energy, energies with respect to the ground state are listed.

TABLE V. Comparison of theoretical[a] and experimental[b] rotational energy levels[c] ($J = 4$).

K	calc(calc-expt)	Expt.	K	calc(calc-expt)	Expt.
Ground state					
0	24.66(−0.01)	24.67	−1	32.10(−0.02)	32.11
+1	33.74(−0.03)	33.77	−2	57.60(−0.07)	57.67
+2	57.63(−0.08)	57.71	−3	98.71(−0.15)	98.86
+3	98.71(−0.15)	98.86	−4	156.20(−0.25)	156.45
+4	156.21(−0.24)	156.45			
4_1					
0	24.54(0.39)	24.15	−1	30.84(0.48)	30.36
+1	32.30(0.52)	31.78	−2	52.73(0.76)	51.97
+2	52.78(0.77)	52.01	−3	88.49(1.16)	87.33
+3	88.49(1.14)	87.35	−4	139.27(1.63)	137.64
+4	139.27(1.62)	137.65			
6_1					
0	24.79(0.55)	24.23	−1	33.39(0.49)	32.90
+1	35.06(0.54)	34.52	−2	62.33(0.48)	61.85
+2	62.36(0.47)	61.89	−3	108.66(0.50)	108.16
+3	108.66(0.48)	108.18	−4	172.62(0.55)	172.07
+4	172.62(0.53)	172.09			
3_1					
0	24.83(0.51)	24.32	−1	32.31(0.59)	31.72
+1	34.05(0.56)	33.49	−2	58.17(0.83)	57.34
+2	58.21(0.82)	57.39	−3	99.83(1.29)	98.54
+3	99.83(1.28)	98.55	−4	158.08(1.94)	156.14
+4	158.08(1.93)	156.15			
2_1					
0	25.06(0.96)	24.10	−1	32.52(1.01)	31.51
+1	34.24(1.11)	33.13	−2	58.22(1.33)	56.89
+2	58.26(1.33)	56.93	−3	99.62(1.80)	97.82
+3	99.62(1.80)	97.82	−4	157.51(2.46)	155.05
+4	157.52(2.47)	155.05			
4_2					
0	24.43		−1	30.29	
+1	31.60		−2	50.45	
+2	50.51		−3	83.23	
+3	83.23		−4	129.69	
+4	129.69				
$4_1 6_1$					
0	24.65		−1	30.77	
+1	32.14		−2	52.62	
+2	52.66		−3	89.64	
+3	89.64		−4	143.33	
+4	143.34				

[a] Results obtained with $N_{max} = 6$ and $K_{max} = 10$.
[b] From the molecular constants reported in Ref. 21.
[c] Relative energy to rotationless origin. See Table IV for these origins.

some $|2-\rangle|000001)$ through this standard Coriolis interaction. Note the standard Coriolis interaction involves essentially only vibrational mixing since only states with the same rotational K label (but opposite Wang phase) are mixed. Different K label mixing, i.e., rotational mixing, can arise from a second Coriolis interaction effect sometimes called[22] accidental Coriolis interaction. The full rovibrational state in the 4_1 band of Table VI is an example of this. This state involves, of course, $|4+\rangle|000100)$ and, through standard Coriolis interaction $|4-\rangle|000001)$. However, we also see a reasonably significant amount of $|2-\rangle|000001)$ and $|2+\rangle|000100)$. Keep in mind the soft-bracketed states have already included molecular asymmetry effects so that this mixing must arise from Coriolis interaction. One way to understand this mixing is to note that there will be a finite Coriolis matrix element between, say, the $|4+\rangle|000100)$ and $|2-\rangle|000001)$ states owing to the presence of minor primitive components:

$$(4+|(000100|W|000001)|2-) \approx a\langle 2+|\langle 000100|W|00001\rangle|2-\rangle.$$

In the above equation we have used the fact (see Table II) that $|4+\rangle|000100)$, through the asymmetry coupling included in its definition, includes a small amount of the primitive state $|2+\rangle|000100\rangle$. Actually, for such simultaneous vibration and rotation mixing to really be noticeable, one needs not only a finite Coriolis coupling between the relevant states, but reasonably close proximity in terms of zero-order

TABLE VI. Eigenstate decompositions of selected rovibrational eigenstates ($J = 16$).

K	Relative E(cm^{-1})[a]	Decomposition[b]		
4_1 band[c]				
0	323.5	0.99| 0)|000100)		
+1	344.1	0.98|1 +)|000100)	−0.15|1 −)|000001)	
+2	364.3	0.97|2 +)|000100)	−0.21|2 −)|000001)	
+3	395.3	0.94|3 +)|000100)	−0.29|3 −)|000001)	+0.12|1 −)|000001)
+4	445.0	0.85|4 +)|000100)	−0.37|4 −)|000001)	−0.34|2 −)|000001)
		−0.11|2 +)|000100)		
+5	512.3	0.90|5 +)|000100)	−0.41|5 −)|000001)	
+6	593.8	0.89|6 +)|000100)	−0.46|6 −)|000001)	
+7	690.1	0.87|7 +)|000100)	−0.49|7 −)|000001)	
+8	802.5	0.86|8 +)|000100)	−0.51|8 −)|000001)	
4_2 band[d]				
0	324.3	0.99|0)|000200)		
+1	345.2	0.98|1 +)|000200)	−0.16|1 −)|000101)	
+2	366.0	0.96|2 +)|000200)	−0.23|2 −)|000101)	
+3	393.9	0.93|3 +)|000200)	−0.33|3 −)|000101)	
+4	439.5	0.88|4 +)|000200)	−0.41|4 −)|000101)	−0.12|4 +)|000002)
+5	499.0	0.70|5 +)|000200)	−0.45|3 −)|000101)	−0.40|5 −)|000101)
		−0.24|3 +)|000002)	−0.21|3 +)|000200)	−0.14|5 +)|000002)
		+0.10|1 +)|000002)		
+6	576.0	0.82|6 +)|000200)	−0.51|6 −)|000101)	−0.20|6 +)|000002)
+7	666.4	0.78|7 +)|000200)	−0.55|7 −)|000101)	−0.23|7 +)|000002)
		−0.12|7 −)|000200)		
+8	772.2	0.76|8 +)|000200)	−0.57|8 −)|000101)	−0.24|8 +)|000002)

[a] Energy relative to rotationless origin.

[b] Eigenstates of the full Hamiltonian are presented in terms of eigenvectors of the unperturbed Hamiltonian H_0, where Coriolis terms are excluded. Eigenvectors of H_0 are described by their leading configuration, $|K+/-)|n_1 n_2 n_3 n_4 n_5 n_6)$, where $|K+/-)$ is the Wang rotational function and $|n_1 n_2 n_3 n_4 n_5 n_6)$ is the zero-order vibrational state.

[c] Rotationless origin was calculated to be 1166.4 cm^{-1} (Table IV).

[d] Rotationless origin was calculated to be 2323.7 cm^{-1} (Table IV).

energies. Table II shows that the $|4+)|000100)$ and $|2-)|000001)$ states lie within 20 cm^{-1} of one another. Actually it is this latter aspect—the closeness of zero-order states—that is the source of the terminology accidental Coriolis interaction.[22] Perhaps a more appropriate term would be secondary Coriolis interaction, since it arises from some kind of prediagonalization scheme and can be thought of as a second order effect.

The above accidental or secondary Coriolis interaction in the 4_1 band might seem relatively minor. Indeed, the experimental consequences of it are small and include, for example, "anomalously large" splittings between $K = +4$ and $K = -4$ rovibrational states of 8000 MHz or 0.3 cm^{-1} [22] in the 4_1 band. A more significant secondary Coriolis effect is seen in the 4_2 band of Table VI. In particular, notice the $K = +5$ full rovibrational state which involves less than 50% ($C = 0.70$; $C^2 = 0.49$) of the zero-order state $|5+)|000200)$. Mixed in with this state are a number of other states such as $|3-)|000101)$, $|5-)|000101)$, and $|3+)|000002)$. Thus, we see a very significant form of simultaneous vibration and rotation mixing, with 4_2 being significantly contaminated by $4_1 6_1$, while both $K = 5$ and 3 rotational states coexist. Within the picture based on a decomposition of H as $H_0 + W$ it is actually a little difficult to see the origin of such mixing. For example, a glance at Table II will show that the zero-order states $|5+)|000200)$ and $|3-)|000101)$ do not include any primitive states with $|C| > 0.10$ that actually would lead to a finite Coriolis matrix element between them. However, these states do include states with $|C| < 0.10$ and this, coupled with the fact that they are reasonably close in energy (about 30 cm^{-1} apart) must lead to the observed result. However, it would be nice if there were a more obvious way to explain such pronounced mixing. In the following subsection we will advance two explanations, one being quantum mechanical and involving a new zero-order representation and the other being classical or semiclassical that involves the idea of nonlinear resonance as suggested by Gray and Davis.[6]

Before going on to a more detailed analysis of the 4_2 case, we should point out that other low-lying vibrational states are similarly affected. For example, the $K = +5$, 4_2 state of Table VI is just one member of two pairs of nearly degenerate and highly mixed states. That is, there is a state which could be labeled $K = -5$ (roughly, all opposite Wang phases) which is nearly degenerate with the $K = +5$ state. About 4.5 cm^{-1} above this "K doublet" is another K doublet, this time corresponding to $|3+/-)|000101)$ being the dominant, but by no means the sole configuration. In fact this slightly higher lying doublet contains significant contamination from $|5-/+)|000200)$ and

$|3-/+\rangle|000002)$. Thus the real signature of the resonance mixing of vibration and rotation in this case is two nearly degenerate K doublets separated by about 4.5 cm^{-1} from one another. The 6_2 vibrational states also show evidence of the resonance mixing discussed here, although not to the same degree.

C. Analysis of Coriolis interactions in the 4_2 level

Consider the following new zero-order Hamiltonian operator:

$$H^0_{vc} = H_{vib} + W + \sum_{K+/-} |J;K^{+/-}\rangle E^{+/-}_{JK} \langle J;K^{+/-}|, \tag{12}$$

where the $E^{+/-}_{JK}$ denote the diagonal matrix elements of H_{rot} in the Wang basis. H^0_{vc} explicitly includes Coriolis coupling W, and molecular asymmetry (off-diagonal matrix elements in K due to H_{rot}) has been explicitly removed. (Centrifugal effects are understood to be neglected here; as we have seen, their effect on the low vibrational states is very minor.) Such a zero-order Hamiltonian is a quantum mechanical and anharmonically generalized version of the basic "Coriolis adapted normal modes" idea introduced by Burleigh and co-workers.[4] Diagonalization of Eq. (12) with our primitive normal mode/Wang basis set will lead to a set of new zero-order states which we will denote, for simplicity, by $|K+/-]\,|n_1,n_2,n_3,n_4,n_5,n_6]$. As with the soft-bracketed notation used for the states of H_0, an eigenstate of Eq. (12) with such a label will contain, as major component, the primitive state $|K+/-\rangle|n_1,n_2,n_3n_4,n_5,n_6\rangle$. In particular, it is the case that strong standard a-axis Coriolis coupling will mix significantly the zero-order states $|5+/-\rangle|000200\rangle$ and $|5-/+\rangle|000101\rangle$. There will in turn be two degenerate pairs of zero-order states of Eq. (12), one pair of which—the lower lying one—can be denoted by $|5+/-]|000200]$. These states contain $|5+/-\rangle|000200\rangle$ as major primitive component, but also about 25% of the $|5-/+\rangle|000101\rangle$ primitive component. It so happens that this pair of states of Eq. (12) will lie accidentally close to the states $|3+/-]|000101]$. Now imagine including the off-diagonal couplings ($\Delta K = 2$) due to H_{rot}. It is then easy to see how the $|5+/-]|000200]$ and $|3+/-]|000101]$ states will be coupled. In terms of the primitive states, this means $|5-/+\rangle|000200\rangle$, $|5+/-\rangle|000101\rangle$, and $|3+/-\rangle|000101\rangle$ will be mixed. The $K=+5$ state in Table VI corresponds to the lower sequence of signs in these three coupled primitive states. We have explicitly verified this mechanism applies in the case of the reduced dimension model to be discussed below.

In order to understand the specific details of the simultaneous vibration and rotation mixing observed in the 4_2 band, detailed quantum mechanical arguments such as those above are essential. However, to understand qualitative features, classical and semiclassical ideas can be highly instructive. Consider Fig. 1. Here we plot in the top panel dE_K/dK vs K, inferred from an analysis of the $J=16$ asymmetric rotor states. Specifically, we took the sequence of rotational levels corresponding to the $|J=16;K^+\rangle|000200)$ states of H_0, fit a cubic spline through these points, and plotted the corresponding derivatives. dE_K/dK may be thought of as a rotational frequency ω_K. Two horizontal lines are also shown in this top panel. These lines correspond to $\Delta\Omega$ and $\Delta\Omega/2$, where $\Delta\Omega$ is the energy difference (divided by $\hbar$) between the $4_1 6_1$ and 4_2 $J=0$ vibrational eigenstates. This frequency, in the limit of a harmonic model, corresponds to the difference in normal mode frequencies between modes 6 and 4. The actual value (102.8 cm^{-1}) of $\Delta\Omega$, however, is larger than the value from the zero-order normal mode frequencies, 81.1 cm^{-1}, and reflects anharmonic effects and other small effects (e.g., the vibrational angular momentum term and Watson term). Interestingly, the $K=5$ region, the region of significant Coriolis induced vibration and rotation mixing, occurs near the intersection of the $\Delta\Omega/2$ and ω_K curves. This represents a 2:1 resonance condition

$$2\omega_K = \Delta\Omega, \tag{13}$$

similar to that seen classically (and quantum mechanically,

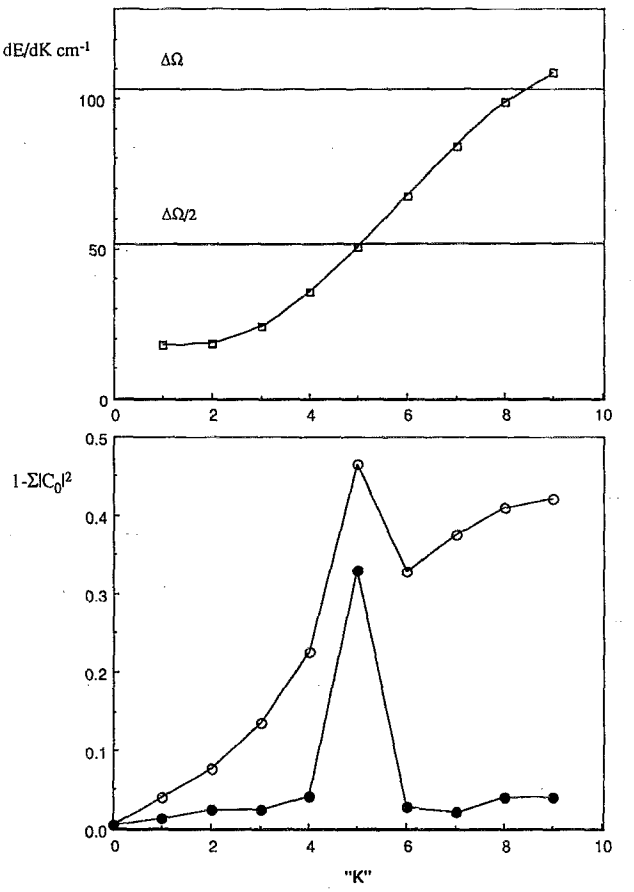

FIG. 1. Upper panel: effective rotational frequency $\omega_K = dE/dK$ inferred from the full dimensional quantum calculations (curve with open squares), and the effective vibrational frequency difference $\Delta\Omega$ (upper horizontal line) and $\Delta\Omega/2$ (lower horizontal line). Lower panel: the vibrational state mixing [Eq. (14); open circles] and the K state mixing [Eq. (15); filled circles]. See the text for additional details.

but with a reduced dimension model) by Gray and Davis[6] for a slightly different (and less satisfactory) potential surface. Such a resonance condition translates into a zero-order near degeneracy of the corresponding quantum mechanical energy levels (of H_0, say) that is subsequently broken by the Coriolis interaction term when a second-order (or matrix) calculation is performed as discussed in the above paragraph. However, it is also instructive to examine the classical limit of Eq. (13). Such frequency matching, combined with Coriolis interaction W, leads to classical resonance zones in classical mechanics where there is the possibility of significant mixing. The reduced dimension classical and quantum studies we also present towards the end of this section further corroborate this viewpoint. One might expect that the 1:1 resonance condition, which would occur near $K=9$, might also be important. Such a resonance condition would link states differing (in a semiclassical limit) by rotational energy $\hbar\omega_K$, which corresponds to mixing of K and $K+1$ states. The coupling between such states is, however, exceedingly small in the vibrational states considered here, since it can arise only from the centrifugal effects in $H_{\rm rot}$ and the b- and c-axis Coriolis couplings. To further point out the interesting connection of such a frequency matching with the quantum mechanics, consider the bottom panel of Fig. 1. Here we show

$$1-\sum_{i,K'}|C_{iK'}|^2 \quad (i\neq|000200\rangle), \tag{14}$$

as open circles, which is a measure of the amount of vibrational mixing induced by Coriolis coupling. The filled circles correspond to

$$1-\sum_{i,K'}|C_{iK'}|^2 \quad (K'\neq K), \tag{15}$$

which is a measure of rotational mixing (K mixing) induced by Coriolis coupling. [The C's in the above two equations come from the expansion Eq. (8).] It can be seen that both functions become sharply peaked in the vicinity of $K=5$, reflecting again the role of the resonance. As seen in Fig. 1, the amount of vibrational mixing, apart from the resonance bumps, increases monotonically. This is because the a-axis Coriolis coupling between specific vibrational states, i.e., 4_2 and $4_1 6_1$ in the present case, is proportional to $|K|$.

In order to solidify the nonlinear resonance idea noted above, it is worthwhile to introduce a reduced dimension Hamiltonian $H_{\rm red}$ that involves only modes 4,6 and rotation analogous to the Hamiltonians of Burleigh and co-workers[4] and Gray and Davis.[6] Actually, there have been many useful theoretical studies of rotation–vibration dynamics based on such simplified models.[4,6–11] In order to describe semiquantiatively the relevant quantum states, however, we have found it is essential to adiabatically correct for the presence of the other normal modes. The relevant analysis and the form of the new reduced dimension Hamiltonian are given in the Appendix. One may determine the rovibrational eigenstates of $H_{\rm red}$ in a manner similar to the full rovibrational state analysis, except now the primitive basis set involves only $|K+/-\rangle|n_4,n_6\rangle$. The corresponding calculations are therefore almost trivial in terms of computational time, involving matrices on the order of 300×300 or 400×400. Table VII displays the rovibrational eigenstates of the reduced dimension Hamiltonian corresponding to some of the full rovibrational eigenstates in Table VI. It is clear that there is quite reasonable agreement, especially in terms of the zero-order state mixing. We should also note that, as in the full dimension calculations, there is actually a $K=-5$ state very close in energy (<0.5 cm^{-1}) to the $K=+5$ state shown in Table VII and, moreover, there is another such K doublet corresponding to states with $|3+/-)|11)$ [and to a lesser extent $|5+/-)|20)$ and $|3-/+)|02)$] being dominant. The energy splitting between the two doublets is about 4.7 cm^{-1}, in good agreement with the exact full dimension result of 4.5 cm^{-1}. We feel justified in asserting this model reproduces the essential quantal aspects of the rotational excitations of the 4_2 state. We should perhaps comment on a slight difference here in relation to the previously studied reduced dimension model.[6] The previous model led to the most significant classical and quantal mixing in the

TABLE VII. Eigenstate decompositions of selected rovibrational eigenstates ($J=16$) of the reduced dimension model.

K	Relative E (cm^{-1})[a]	Decomposition[b]			
4_2 band					
0	326.5	$0.99\|0)\|20)$			
+1	347.0	$0.99\|1+)\|20)$			
+2	363.7	$0.94\|2+)\|20)$	$-0.27\|2-)\|11)$		
+3	392.0	$0.91\|3+)\|20)$	$-0.38\|3-)\|11)$		
+4	437.4	$0.87\|4+)\|20)$	$-0.46\|4-)\|11)$	$-0.14\|2+)\|20)$	$-0.10\|1+)\|20)$
+5	497.8	$0.74\|5+)\|20)$	$-0.49\|5-)\|11)$	$-0.30\|3-)\|11)$	
		$-0.23\|3+)\|20)$	$-0.16\|5+)\|02)$	$-0.15\|3+)\|02)$	
+6	575.1	$0.80\|6+)\|20)$	$-0.55\|6-)\|11)$	$-0.19\|6+)\|02)$	
+7	667.5	$0.77\|7+)\|20)$	$-0.59\|7-)\|11)$	$-0.22\|7+)\|02)$	
+8	775.5	$0.75\|8+)\|20)$	$-0.61\|8-)\|11)$	$-0.24\|8+)\|02)$	

[a] Energy relative to the rotationless origin.

[b] Eigenstates of the reduced dimension Hamiltonian are presented in terms of eigenvectors of the unperturbed Hamiltonian H_0, where Coriolis terms are excluded. Eigenvectors of H_0 are described by their leading configuration, $|K+/-)|n_4 n_6)$, where $|K+/-)$ is the Wang rotational function and $|n_4 n_6)$ is the vibrational zero-order state.

$K = 2$–4 regime. The new model, based on the more accurate potential surface and, most importantly, including the adiabatic effects of the other normal modes, leads to the $K = 3$–5 regime as being most mixed, in agreement with the present full dimension quantum rovibrational states.

To illustrate how this mixing really is a classical effect, we note that it is easy to write down a classical analog of $H_{\rm red}$. One simply replaces the corresponding normal coordinate position and momentum operators with canonically conjugate classical position and momentum variables. Following Gray and Davis[6] (see also Ezra[11]), one replaces the total angular momentum components J_α with their classical counterparts which involve an angle variable q_K and its canonically conjugate momentum K. K is the (classical) projection of J on the z (or a) body-fixed axis. The result is a classical Hamiltonian $H_{\rm red} = H_{\rm red}(Q_4,P_4,Q_6,P_6,q_K,K)$ which corresponds to a three degree of freedom problem. Actually, this Hamiltonian can be considerably simplified by two canonical transformations and an averaging procedure. The basic idea is one defines new vibrational action variables v_4 and v_6 (which are proportionate to the zero-order normal mode energies and may be thought of as the classical analogs of the quantum numbers n_4 and n_6), along with their associated angle variables q_4 and q_6. Then one realizes that the variable $I_+ = v_4 + v_6$ rapidly oscillates about a mean value and, to a reasonable approximation, I_+ is constant. Thus one performs a final canonical transformation to new sum and difference action variables I_+ and $I_- = v_4 - v_6$, and their corresponding angle variables q_+ and q_-. Finally, one averages over the fast variable q_+ to obtain an even more reduced dimension Hamiltonian $H_{\rm red}(q_K,K,q_-,I_-;I_+)$. Since q_+ does not occur in this final Hamiltonian, I_+ is a constant of the motion and we have a two degree of freedom model. For a total energy near the $K = +5$ eigenstate we have examined the classical phase space of this Hamiltonian. The resulting Hamiltonian is very similar in form to that in Ref. 6, although the parameters are somewhat different (see the Appendix). Figures 2(a) and 2(b) display two surfaces of section[23] corresponding to an energy close to the $K = +5,4_2$ state of Table VII, and with $I_+ = 2$ and $J = 16$. In Fig. 2(a) we have run a number of classical trajectories and plotted q_k and K for each trajectory whenever q_- passed through 0. The large islands centered on about $(q_k,K) = (0.5,3.5)$ and $(3.8,3.5)$ represent the 2:1 nonlinear resonance. Note a single resonance island region connects $K = 3$ and 5 and has an area on the order of Planck's constant h ($= \pi$ in the atomic units employed in the figure). Figure 2(b) also shows the corresponding surface of section for (q_-,I_-). Here we have plotted (q_-,I_-) every time trajectories have passed through $q_k = 1$ and have displayed only those trajectories that lie within the resonance island. Again, large islands of area on the order of h are seen. Notice I_- ranging between -2 and 3 corresponds to significant vibrational mixing as well. For example, when $I_- = 0$ corresponds to classical vibrational actions $(v_4,v_6) = (1,1)$ and $I_- = 2$ corresponds to (2,0). While we have not attempted a semiclassical quantization[24] of the reduced dimension model, the evidence of the two surfaces of section shown is that phase space

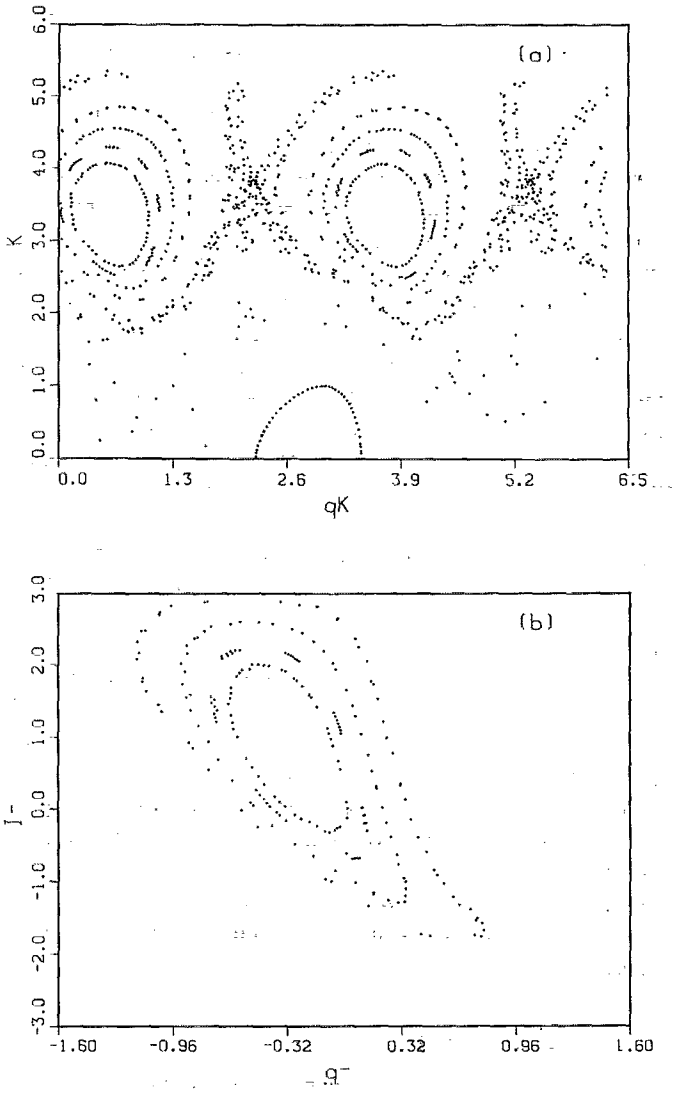

FIG. 2. Surfaces of section for an absolute energy of 3994 cm^{-1} and $J = 16$ in the two degree of freedom reduced dimension model discussed in the text. $I_+ = 2$ in these calculations corresponding to the 4_2 and $4_1 6_1$ vibrational energy regime. This total energy corresponds to 503 cm^{-1} in the relative energy units of Table VI and is therefore in the region where the simultaneous vibration–rotation mixing is observed. (a) (q_K,K) surface of section, as defined in text. Note only the positive K portion is displayed, with a similar negative K portion being understood to exist. (b) (q_-,I_-) surface of section. Note the range of q_- may be taken to be $[-\pi/2,\pi/2]$.

volumes of sufficient size exist to define resonance states and that the strong accidental or secondary Coriolis interaction has a clear classical analog. The small (4.7 cm^{-1}) splitting between K doublets in the resonance zone is probably due to tunneling and would also be interesting to explore further.

IV. DISCUSSION AND SUMMARY

In this paper we have presented accurate, variationally determined rovibrational energy levels for formaldehyde in the limit of low vibrational excitations. The method of calculation (Sec. II) featured the use of an iterative matrix diagonalization algorithm[17] that permitted rather large matrices to be considered. Results for $J = 0$, 4, and 16 were

presented in Sec. III and compared with experiment and/or other theoretical calculations, where available. We also saw that there can be particular instances of simultaneous vibration and rotation mixing in the high total angular momentum but relatively low vibrational energy regime of full mode formaldehyde. This mixing was in turn associated with certain resonance conditions being satisfied. In particular, the importance of the matching of the frequency difference between modes 6 and 4 with multiples of the rotational frequency, should be noted as an important source of simultaneous vibration and rotation mixing. It should be noted that, in a certain sense, more standard techniques of spectroscopic analysis could also be invoked to explain this mixing. For example, one can refer to the existence of certain accidental degeneracies (perhaps viewed in terms of a zero-order, "Coriolis adapted" picture[4] as noted in Sec. III C) and their mixing through degenerate perturbation theory. The resonance interpretation, however, is useful because of the underlying classical mechanism of energy transfer that it suggests and represents an alternative way of thinking about such mixing.

It should also be noted that similar types of resonance effects as seen in this paper have been found to be quite important in understanding the higher lying rovibrational states. For example, the rovibrational states originating from the 4_3 vibrational level are significantly coupled through a-axis Coriolis coupling to the $4_2 6_1$, $4_1 6_2$, and 6_3 vibrational states. Studies concerning such higher rovibrational states, where one must also consider b,c-axis Coriolis interactions as an important source of mixing, will be reported separately.[25]

ACKNOWLEDGMENTS

We wish to thank E. L. Sibert for many helpful conversations and for communicating to us his potential surface. This work was supported by the Office of Basic Energy Sciences, Division of Chemical Sciences, U.S. Department of Energy, under Contract No. W-31-109-ENG-38.

APPENDIX: NEW REDUCED DIMENSION MODEL

In previous work[4,6] a three degree of freedom, or reduced dimension model was introduced to explain qualitative aspects of how modes 4 and 6 in formaldehyde interact with rotation. This model was constructed simply by neglecting all the other modes and their couplings to modes 4,6 and rotation. Actually, it is not difficult to construct a better reduced dimension model, which is also more logical, by adiabatically averaging the full Hamiltonian over the other four modes. The resulting model leads to eigenstates in surprisingly good accord with the full dimensional ones and its classical dynamics shows the importance of nonlinear resonance between modes 4,6 and rotation, as discussed in the main text.

Our concern is with the subset of rovibration states of formaldehyde at relatively low vibrational excitation energy that are characterized by (i.e., have as their major components) zero-order normal mode states with $n_1 = n_2 = n_3 = n_5 = 0$. Table I shows that the frequencies corresponding to these modes are all greater than those for modes 4 and 6 (and rotation) so that a plausible reduced dimension Hamiltonian model can be obtained by adiabatically averaging over modes 1, 2, 3, and 5:

$$H_{\rm red}(Q_4,P_4,Q_6,P_6,J) = \langle 0000|H|0000\rangle_{1,2,3,5}, \quad \text{(A1)}$$

where H is the full Hamiltonian operator and $|0000\rangle$ denotes the zero-order (and zero-point) product of normal mode states 1, 2, 3, and 5. Equation (A1) will still lead to a rather complicated Hamiltonian, although one dependent on just three degrees of freedom, the two vibrations 4,6 interacting with rotation J. For the purposes of presenting the simplest model that essentially reproduces all the effects we are interested in, we invoke three additional assumptions:

(i) Potential terms up to fourth order only in normal coordinates will be considered. This is reasonable in view of the relatively low vibrational excitations of interest.

(ii) Centrifugal effects will be neglected. Thus the $H_{\rm rot}$ part of Eq. (A1) becomes a simple, asymmetric top Hamiltonian. As noted in the text, centrifugal effects turn out to be quite minor for the states of interest in this paper.

(iii) The purely quantum (and small) Watson correction term in H will be neglected, as well as the result of adiabatic averages such as $\langle 0|Q_iP_i|0\rangle$, where $i = 1$, 2, 3, or 5. Note that in a simple correspondence principle limit, $\langle 0|Q_iP_i|0\rangle$ is zero. Thus this approximation is tantamount to neglecting all purely quantal corrections to the adiabatic average.

We should stress that none of the above approximations are essential and that relaxing any of them leads only to slight shifts in the energy levels. Incidentally, this fact is one measure of the robustness of the resonance phenomena of interest to us here.

In carrying out the adiabatic analysis we should point out that it is important to carefully include the result of averaging over the rotational kinetic energy,

$$\tfrac{1}{2}\sum_\alpha (J_\alpha - \Pi_\alpha)^2 \mu^0_{\alpha\alpha}. \quad \text{(A2)}$$

Equation (A2) leads, first, to the asymmetric rotor Hamiltonian:

$$H^0_{\rm rot} = \tfrac{1}{2}\sum_\alpha \mu^0_{\alpha\alpha} J^2_\alpha. \quad \text{(A3)}$$

Equation (A2) also leads to the important Coriolis coupling term

$$W = -K\mu^0_{zz}\xi^z_{46}(Q_4P_6 - Q_6P_4), \quad \text{(A4)}$$

with K being used to represent the operator J_z. The three Π^2_α terms of Eq. (A2), keeping in mind approximation (iii) above, lead to the adiabatic correction

$$a_4Q_4^2 + a_6Q_6^2 + b_4P_4^2 + b_6P_6^2,$$

where the a_i and b_i arise from adiabatically averaging over $Q_i^2P_j^2$ and $Q_j^2P_i^2$ terms, respectively. For example, since (Table I) ξ^x_{16}, ξ^x_{26}, and ξ^x_{36} ($x = c$ axis) are all nonzero,

$$a_6 = \frac{\mu^0_{xx}}{2}\left[(\xi^x_{16})^2\langle 0|P_1^2|0\rangle + (\xi^x_{26})^2\langle 0|P_2^2|0\rangle + (\xi^x_{36})^2\langle 0|P_3^2|0\rangle\right]. \quad \text{(A5)}$$

The final result is

$$H_{\rm red} = \tfrac{1}{2}(P_4^2 + P_6^2) + H^0_{\rm rot} + \sum_{i=4,6} A_{ii}Q_i^2 + A_{iiii}Q_i^4 + A_{4466}Q_4^2Q_6^2 + b_4P_4^2 + b_6P_6^2 + W, \quad \text{(A6)}$$

where, e.g.,

$$A_{66} = V_{66} + \sum{}' V_{ii66}\langle 0|Q_i^2|0\rangle + a_6, \quad \text{(A7)}$$

with the prime on the sum implying not to include $i = 4$ or 6 and V_{ijkl} being the original potential coefficient for $Q_iQ_jQ_kQ_l$.

Perhaps the most significant part (in relation to previous treatments) is the new effective frequencies that arise out expressions such as Eq. (A7):

$$\omega_4^{\rm eff} = (2A_{44})^{1/2} = 1117.3\ \text{cm}^{-1},$$
$$\omega_6^{\rm eff} = (2A_{66})^{1/2} = 1220.3\ \text{cm}^{-1}. \quad \text{(A8)}$$

Note that the effective frequency difference is then 103.0 cm^{-1} in good agreement with the full dimension calculation estimate (based on the $4_1 6_1$ and 4_2 energy level differences, cf. Fig. 1) of 102.8 cm^{-1}. Actually, the precise agreement here is partly fortuitous: if one also includes the P_4^2 and P_6^2 correction terms in estimating the effective frequencies of the reduced dimension model, the effective frequency difference then becomes 101.6 cm^{-1}, which differs a little more from the full dimension result. The effective frequency difference should also be compared with the frequency difference without any adiabatic corrections, 81.1 cm^{-1}.

The parameters in Eq. (A6) are, in atomic units: $A_{44} = 1.295\,73\times10^{-5}$, $A_{66} = 1.545\,66\times10^{-5}$, $b_4 = 1.504\,15\times10^{-3}$, $b_6 = 2.188\,61\times10^{-4}$, and $A_{4466} = 1.450\,638\times10^{-8}$, $A_{4444} = 7.774\times10^{-10}$, $A_{6666} = 6.266\times10^{-10}$.

[1] H. L. Dai, C. L. Korpa, J. L. Kinsey, and R. W. Field, J. Chem. Phys. **82**, 1688 (1985).
[2] J. G. Haub and B. J. Orr, J. Chem. Phys. **86**, 3380 (1987).
[3] F. W. Farley, L. V. Novakoski, M. K. Dubey, G. M. Nathanson, and G. M. McClelland, J. Chem. Phys. **88**, 1460 (1988).
[4] D. C. Burleigh, R. C. Mayrhofer, and E. L. Sibert, J. Chem. Phys. **89**, 7201 (1988).
[5] E. L. Sibert, J. Chem. Phys. **90**, 2672 (1989).
[6] S. K. Gray and M. J. Davis, J. Chem. Phys. **90**, 5420 (1989).
[7] W. J. Hovingh and R. Parson, Chem. Phys. Lett. **158**, 222 (1989).
[8] J. H. Frederick and G. M. McClelland, J. Chem. Phys. **84**, 4347 (1986).
[9] T. Uzer, G. A. Natanson, and J. T. Hynes, Chem. Phys. Lett. **122**, 12 (1985).
[10] (a) D. K. Sahm and T. Uzer, J. Chem. Phys. **90**, 3159 (1989); (b) D. K. Sahm, S. W. McWhorter, and T. Uzer, *ibid.* **91**, 219 (1989); (c) D. K. Sahm and T. Uzer, Chem. Phys. Lett. **163**, 5 (1989).
[11] G. S. Ezra, Chem. Phys. Lett. **127**, 492 (1986).
[12] M. Aoyagi, S. K. Gray, and M. J. Davis, J. Opt. Soc. Am. B **7**, 1859 (1990).
[13] R. J. Whitehead and N. C. Handy, J. Mol. Spectrosc. **55**, 356 (1975).
[14] J. K. G. Watson, Mol. Phys. **15**, 479 (1968).
[15] H. Romanowski, J. M. Bowman, and L. B. Harding, J. Chem. Phys. **82**, 4155 (1985).
[16] D. Huber, Int. J. Quantum Chem. **28**, 245 (1985).
[17] (a) E. R. Davidson, J. Comp. Phys. **17**, 87 (1975); (b) E. R. Davidson, in *Methods in Computational Molecular Physics*, edited by G. H. F. Diercksen and S. Wilson (Reidel, Dordrecht, Holland, 1982), p. 95.
[18] J. Tennyson, Comput. Phys. Rep. **4**, 1 (1986).
[19] B. N. Partlett, *The Symmetric Eigenvalue Problem* (Prentice-Hall, Englewood Cliffs, NJ, 1980).
[20] D. E. Reisner, R. W. Field, J. L. Kinsey, and H.-L. Dai, J. Chem. Phys. **80**, 5968 (1984).
[21] M. Allegrini, J. W. C. Johns, and A. R. W. McKellar, J. Mol. Spectrosc. **67**, 476 (1977).
[22] T. Nakagawa and Y. Morino, J. Mol. Spectrosc. **38**, 84 (1971).
[23] See, for example, A. J. Lichtenberg and M. A. Lieberman, *Regular and Stochastic Motion* (Springer, New York, 1983).
[24] (a) D. W. Noid, M. L. Koszykowsky, and R. A. Marcus, Annu. Rev. Phys. Chem. **32**, 267 (1981); (b) G. S. Ezra, C. C. Martens, and L. E. Fried, J. Phys. Chem. **91**, 3721 (1987).
[25] M. Aoyagi, J. Chem. Phys. (to be submitted).